

Supplemental Online Material

**Caspase-1–mediated pathway promotes generation
of thromboinflammatory microparticles**

**Andrea S. Rothmeier, Patrizia Marchese, Brian G. Petrich, Christian Furlan-
Freguia, Mark H. Ginsberg, Zaverio M. Ruggeri, and Wolfram Ruf**

Extended Experimental Procedures

Bone marrow-derived macrophages (BMDM): All animal procedures were performed under protocols approved by the IACUC of the Scripps Research Institute. BMDM were generated from total bone marrow cells isolated from C57BL/6J mice, TF cytoplasmic domain-deleted TF^{ΔCT} mice (1), TF^{fl/fl} *Lysm-Cre* mice (2), caspase 1-deficient mice (3) or human TF knock-in (TFKI) mice (4). Cells were cultured for 7 days in DMEM, 10% FCS, 20% L cell medium, 1 mM L-glutamine, penicillin and streptomycin, as described previously (5). Cells were seeded at 1×10^6 cells/well in a 12-well plate and primed overnight with 100 ng/ml IFN γ (PeproTech). Typically, macrophages were stimulated the next day with 1 μ g/ml LPS (*Salmonella abortus equi*, Enzo Life Sciences) for 4 hours prior to functional characterization.

MP release reaction: Cells were rinsed once in BSS buffer (0.13 M Na-gluconate, 0.02 M HEPES, 5 mM glucose, 5 mM glycine, 5 mM KCl, 1 mM MgCl₂, pH 7.5) and then exposed in the same buffer to 5 mM ATP (Roche Applied Science) for 30 minutes or as indicated. Cells were pretreated for 30 minutes with DNCB (30 μ M, Sigma-Aldrich), auranofin (various concentrations as indicated, Tocris), parthenolide (10 μ M, Cayman Chemicals), BAY11-7082 (12 μ M, Cayman Chemicals), DPI (100 μ M, Sigma-Aldrich), phalloidin oleate (100 nM, EMD Millipore), CASIN (10 μ M, Xcess Biosciences), NFA (30 μ M, Sigma-Aldrich), DIDS (50 μ M, Sigma-Aldrich), and Rofecoxib (10 μ M, Cayman Chemicals), immediately prior to ATP stimulation with PAO (10 μ M, Sigma-Aldrich), filipin (5 μ g/ml, Sigma-Aldrich), ALLN (1 μ M, EMD Millipore, Billerica, MA) or Ac-YVAD-CMK (10 μ M, Enzo Life Sciences), or as indicated with PX-12 (5 and 50 μ M, Tocris). Surface accessible free thiols were labeled with 100 μ M N-(3-maleimidopropionyl)

biocytin (MPB, Cayman Chemical) added at the beginning of the MP release reaction or as indicated. Typically, 6 12-well-plate wells were pooled for Western blot detection of MP and 2 wells pooled in triplicates for functional assays of MP.

Supernatants were cleared from cellular debris by centrifugation for 10' at 1,000 g and MP were collected by centrifugation for 1 hour at 16,000 g at 4 °C. MP were resuspended for functional assay in HBS (10 mM Hepes, pH 7.4, 137 mM NaCl, 5.3 mM KCl, 1.5 mM CaCl₂) or for Western blotting in non-reducing SDS sample buffer (Life Technologies). Proteins in MP-depleted supernatant were precipitated with 30% trichloroacetic acid and the pellet recovered by centrifugation was washed with acetone and resuspended in non-reducing SDS sample buffer supplemented with Tris base to neutralize residual acid.

Functional Assays: TF activity was determined by adding 0.5 nM mouse FVIIa (kindly provided by L. Petersen, Novo Nordisk) and 50 nM FX (Haematologic Technologies) to adherent cells in HBS or by adding 2 nM VIIa and 100 nM FX to MP. The time course of FXa generation was measured at 37 °C using quantification in EDTA quenched samples with the chromogenic substrate Spectrozyme FXa (Sekisui Diagnostics). MP prothrombinase activity was measured in HBS with 10 nM FVa, 5 nM FXa and 500 nM prothrombin (Haematologic Technologies) at ambient temperatures and quantification of thrombin generation with the chromogenic substrate Spectrozyme TH (Sekisui Diagnostics).

Flow chamber experiments: Confocal microscopy and quantitative image analysis were performed as previously described (5) with the following modifications. Stimulation of cells with 5 mM ATP was performed in the mounted flow chamber under

flow for 10 minutes. Subsequently, cells were perfused with recalcified mouse blood that was mixed with procoagulant MP and other reagents, as indicated, immediately prior to perfusion. The wall shear rate was 300 s^{-1} instead of 500 s^{-1} , and the perfused blood contained 200 nM lepirudin to block the activity of thrombin possibly generated during blood manipulation prior to perfusion of the flow chamber. Three-dimensional image reconstruction of cells, platelet aggregates and fibrin deposited on the flow chamber surface was obtained using Volume Viewer in Image J (<http://rsweb.nih.gov/ij/plugins/volume-viewer.html>).

Identification of MP proteins by mass spectroscopy: Cell-free supernatant was concentrated in an Amicon Ultra 3,000 MW and MP were recovered by centrifugation. MP proteins were separated by SDS-PAGE, stained with Coomassie Blue, and single protein bands were isolated based on the location of thiol-labeled bands on adjacent lanes. Gel pieces were destained and extracted, reduced (10 mM DTT), alkylated (55 mM iodoacetamide) and digested with trypsin for identification by nano-LC-MS/MS at The Scripps Research Institute Center for Mass Spectrometry.

Western blotting: We used the following antibodies for detection of proteins by Western blotting. Antibodies generated by us were polyclonal anti-mouse TF (5) or anti-human TF (6), and polyclonal anti-integrin antibodies specific for $\beta 1$ (5). Anti-IL1 β 3ZD was obtained from the National Cancer Institute. The following commercially available antibodies were used: anti-PDI clone BD34 (610947, BD Biosciences), anti- γ -actin (sc-65638), anti-TRXR1 (sc-28321), anti-filamin (H-300, sc-28284), anti-caspase 1 (M-20, sc-514), anti-NLRP3 (cryopyrin, H-66, sc-66846) and anti-TXNIP (anti-VDUP1, D-2, sc-271237) all from Santa Cruz Biotechnology, anti-calpastatin (#4146) and anti-TRX

(#2298) antibodies (Cell Signaling, Boston, MA). SA-HRP (SA-5704) for detection of MPB and PEG-10k was purchased from Vector Laboratories. MP and cells were typically lysed in non-reducing SDS-PAGE sample buffer. For Western-blotting of cellular TF, membrane fractions were prepared by TX-114 phase separation, using repeated extractions in 1% Triton-X114 (0.1 M Tris pH 8.5, 10 mM EDTA, 1 mM PMSF) and acetone precipitation of detergent pellets.

GSH-assay: Stimulated macrophages were rinsed with PBS and lysed in 0.1 M KH_2PO_4 , 0.1 M K_2HPO_4 , 5 mM EDTA, 1% Triton-X100, 25 mM sulfosalicylic acid for 30 minutes on ice. Cell lysates were sonicated and cleared by centrifugation at 1,000 g for 5 minutes at 4 °C). Reduced GSH levels were determined from the difference of total GSH/GSSG concentration and oxidized GSSG in 2-vinylpyridine treated samples, using reduction of 0.5 mM DTNB to TNB as readout in a GSSG assay with 0.5 U/ml glutathione reductase and 0.25 mM β -NADPH. Absorbance of TNB at 405 nm was quantified in a SpectraMax M2 plate reader (Molecular Devices).

DHE-assay: DHE (50 μM) was added 10 minutes after addition of ATP to cells pretreated with or without DNCB (30 μM) and/or DPI (100 μM). Cells were incubated for another 10 minutes in BSS buffer, rinsed once with ice-cold PBS, and gently scraped into 100 μl FACS buffer (PBS, 1 mM EDTA, 1% FCS) and analyzed after 2 washes on a LSR-II flow cytometer (BD Biosciences). Mean fluorescence of reduced DHE was detected in the Pacific Blue channel and of oxidized DHE in the PE-TexasRed channel.

Insulin Turbidity Assay: 10 μM bovine PDI (Sigma Aldrich) was added to 40 mg/ml insulin (Sigma Aldrich) in reaction buffer (0.1 M K_2HPO_4 , 20 mM EDTA, 5 mM

GSH, pH7.0) and incubated in triplicates in the absence or presence of inhibitors at ambient temperature. Absorbance of precipitated insulin was measured at 650 nm.

Annexin 5 Staining: Exposure of phosphatidylserine (PS) was detected by staining adherent cells with FITC-labeled annexin 5 (BD Biosciences) immediately after incubation with ATP in HBS buffer containing 1.5 mM CaCl₂ at ambient temperature. Images were taken with a 10x objective on a Nikon Eclipse Fluorescent microscope. Fluorescence intensity was analyzed using ImageJ (<http://rsweb.nih.gov>).

FACS analysis of MP: For quantification of MP counts by FACS, cell-free supernatants with MP were analyzed on a LSR-II flow cytometer (BD Biosciences) calibrated with a defined platelet suspension for size and number of events, as described (7). After removal of cell debris (10 minutes 1,000 *g* at 4 °C), 66 nM phalloidin-Alexa 633 conjugate (Life Technologies), 5 µg/ml anti-human TF 9C3-Alexa 647 conjugate and 0.5 µg/ml lactadherin-FITC (Haematologic Technologies) were added to MP from human TFKI mice. MP suspensions were incubated for at least 15 minutes on ice and analyzed within 60 minutes of preparation. FACS data were analyzed using FlowJo software (Tree Star).

Confocal microscopy: Cells were seeded at a density of 5×10^5 cells/well in a 12-well plate on glass cover slips, primed with IFN γ overnight and stimulated the next day for 4 hours with LPS in complete medium. Cells were transferred to HBS and incubated for 10 minutes in the dark at ambient temperature with each 5 µg/ml Alexa 647-conjugated anti-TF antibodies 10H10, 5G9, and 9C3 (8) for TFKI macrophages or 0.5 µg/ml affinity-purified rabbit anti-mouse TF antibody. After washes, cells were incubated in BSS buffer with or without ATP (5 mM) for the indicated times. Cells were fixed with

1% formaldehyde in PBS for 10 minutes at room temperature, followed by three rinses before cells were permeabilized with 0.1 % Triton X-100/PBS for 3 minutes.

For F-actin staining, cells were incubated with phalloidin Alexa 488/564/633 (Life Technologies) in 1% BSA in PBS for 30 minutes. For mouse TF labeling, cells were blocked with 5% BSA in PBS after permeabilization and incubated with Alexa Fluor 488 Goat Anti-Rabbit IgG (1:400, Life Technologies) and Alexa 564-Phalloidin (Life Technologies) in 1% BSA in PBS for 30 minutes. Nuclei were counterstained with 1 $\mu\text{g/ml}$ Hoechst 33342 (Life Technologies) and cover slips embedded in Fluorescent Mounting Medium (Dako, Carpinteria, CA).

For MPB-staining, cells were stimulated with ATP for 20 minutes in BSS Buffer and MPB was added to the reaction for the last 5 minutes. Cells were washed with PBS and fixed with 1% formaldehyde in PBS. Afterwards, cells were stained with 25 $\mu\text{g/ml}$ TexasRed-conjugated streptavidin (Vector Laboratories) in PBS pH 8.5 for 30 minutes at room temperature. Nuclei were counter-stained with 100 ng/ml DAPI in PBS containing 0.1% Tween-20.

Confocal images were taken with a 63x oil emersion objective on a Zeiss 710 LSM. Z-stacks were scanned in 21 slices at 0.29 μm thickness. Images were processed with Image Browser (Zeiss) and Imaris (Bitplane) image analysis software. Due to its low fluorescence intensity, brightness and contrast was adjusted separately for the channel of TF-staining. TF localization on filopodia was quantified by determining the total number of TF signals on filopodia and the cell body for 6 individual cells per condition in at least 3 independent experiments.

Statistics: Statistical analysis was performed using Prism 6 software (GraphPad Software). For statistics comparing two groups *t*-test (two-sided) was used and for statistical analysis of more than 2 One Way ANOVA with Bonferroni multiple comparison correction was employed. All analyses were performed on at least three independent experiments and P values of less than 0.05 were considered significant.

Study approval: Animal procedures were approved by the IACUC of the Scripps Research Institute.

Supplemental Figure and Movie Legends

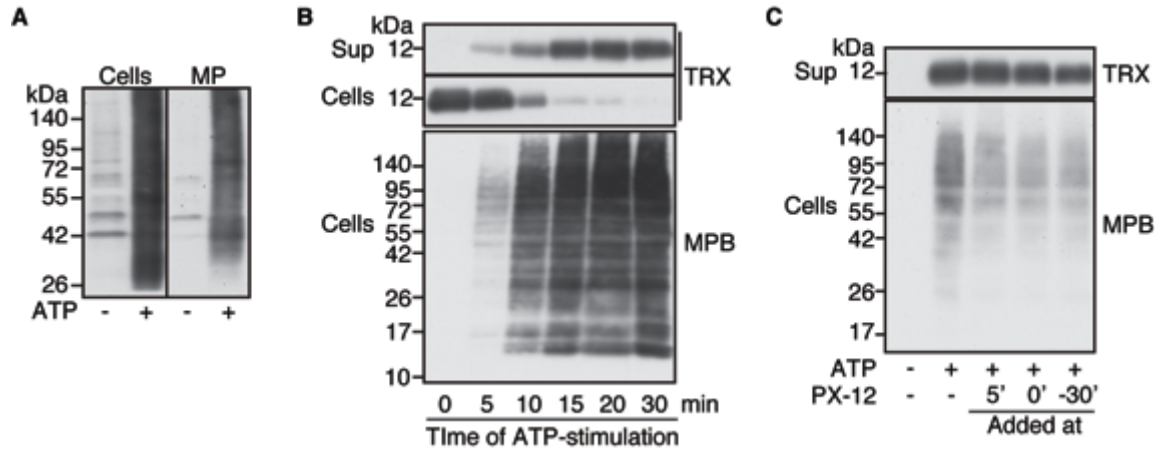


Figure S1: Control experiments for P2RX7 activation-induced extracellular reductive changes. (A) Control and ATP-stimulated cells were labeled with cell impermeable biotin-PEG with a 10 kDa molecular weight. Streptavidin-HRP blots visualize exposure of solvent accessible free thiol residues following ATP-stimulation. (B) Time course of ATP-stimulation-induced TRX release and extracellular reductive changes were detected by Western and streptavidin blotting of MPB-labeled samples. (C) MPB-labeling and TRX-release of macrophages following ATP-stimulation in the presence of low concentrations of the TRX-inhibitor PX-12 (5 μ M) added 5 minutes after, with the start (0') or 30 minutes prior to (-30') stimulation with ATP.

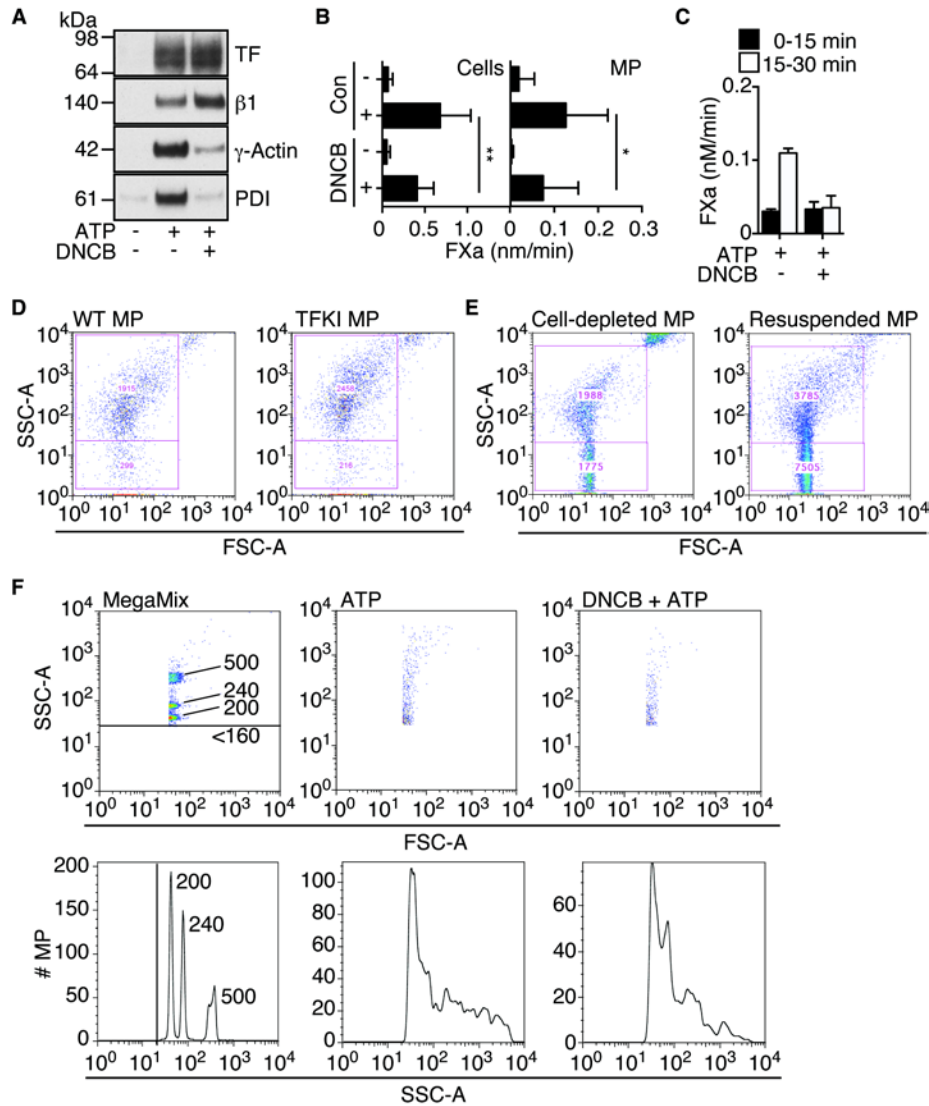


Figure S2: Control experiments to confirm that human TFKI macrophages respond to ATP-stimulation and DNCB-treatment similar to wild-type macrophages. (A) Western blotting for human TF, integrin $\beta 1$, γ -actin and PDI on MP derived from control or DNCB-blocked TFKI macrophages. (B) TF pro-coagulant activity on cells and MP determined by FXa generation assay. (C) Effect of DNCB-treatment on FXa generation by MP collected 0 - 15 minutes (black bars) and 15 - 30 minutes (open bars) following ATP-stimulation of TFKI macrophages. (D) Forward and sideward scatter properties of MP derived from ATP-stimulated WT macrophages (WT MP) or TFKI macrophages (TFKI MP) were similar in FACS analysis. (E) FACS analysis of MP in cell-depleted supernatants from ATP-stimulated TFKI macrophages or MP recovered by centrifugation followed by resuspension (Resuspended MP) shows that MP isolation for functional assays did not appreciably change the appearance of MP, indicating structural integrity following isolation. (F) Size determination of MP derived from TFKI cells using MegaMix calibration beads (160, 200, 240, and 500 nm). Particles smaller than 200 nm were classified as debris and excluded from the analysis.

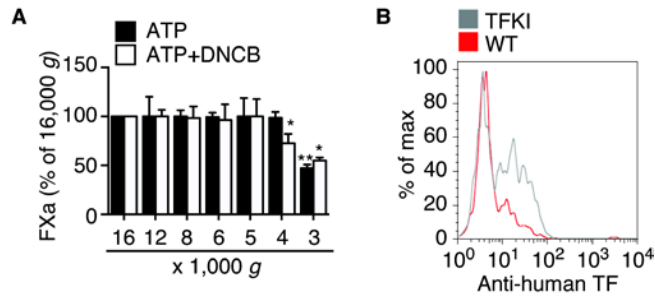


Figure S3: Control experiments for the effects of DNCB-treatment on TF activation and MP generation. (A) FXa generation of MP after collecting MP from ATP stimulated control and DNCB-treated cells at different centrifugation speeds. While procoagulant activity of MP from control cells was fully recovered by centrifugation at 4,000 g, procoagulant activity of MP from DNCB-treated cells was significantly reduced compared to typical collection at 16,000 g, indicating that MP from DNCB-treated cells are smaller in size. (B) Specificity of MP TF staining with anti-human TF antibody 9C3 was demonstrated by lack of staining of MP derived from WT macrophages expressing mouse TF as compared to MP derived from TFKI MP.

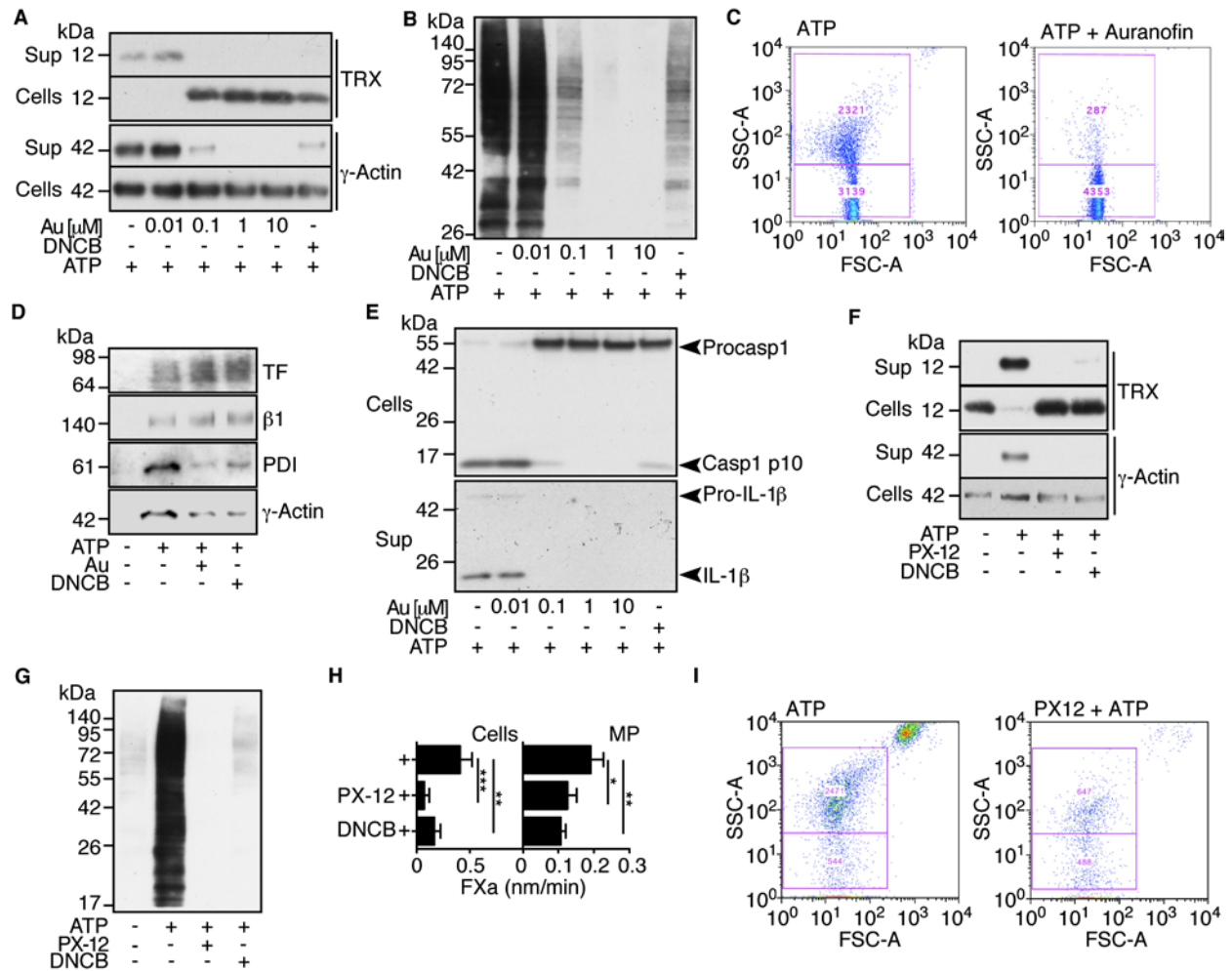


Figure S4: Control experiments for the effects of inhibiting the TRX-TRXR system using the pharmacological inhibitors auranofin and PX-12. (A) Western blots of TRX and γ -actin in cells and MP-free supernatant (Sup) from ATP-stimulated control, different concentrations of TRXR-inhibitors auranofin (Au) or 30 μ M DNCB treated cells. (B) Streptavidin blot of ATP-induced solvent accessible free thiols labeled with MPB in control, auranofin (Au), and DNCB-treated cells. (C) FACS analysis of MP released from TFKI macrophages activated with ATP in the presence or absence of 1 μ M auranofin (Au). (D) Western blots of MP for TF, integrin β 1, PDI and γ -actin demonstrated diminished release of thiol-regulated proteins in auranofin-treated (1 μ M) cells. (E) Western blots of caspase 1 activation and IL-1 β release in ATP-stimulated cells with and without treatment with various concentrations of auranofin (Au) or 30 μ M DNCB. (F) PX-12 is a small molecule inhibitor that oxidizes the vicinal thiols in TRX and – at higher concentrations – competes with the binding to TRXR (9). Western blotting showed that treatment with high concentration (50 μ M) of PX-12 inhibited the release of γ -actin and TRX from ATP-stimulated cells and (G) prevented reductive changes in the extracellular proteome as determined by MPB-labeling and streptavidin blot. (H) ATP-induced TF activity on cells and MP was reduced when cells were treated with PX-12 or DNCB. (I) FACS analysis showed reduced release of characteristic large MP from TFKI cells blocked with high concentrations of PX-12.

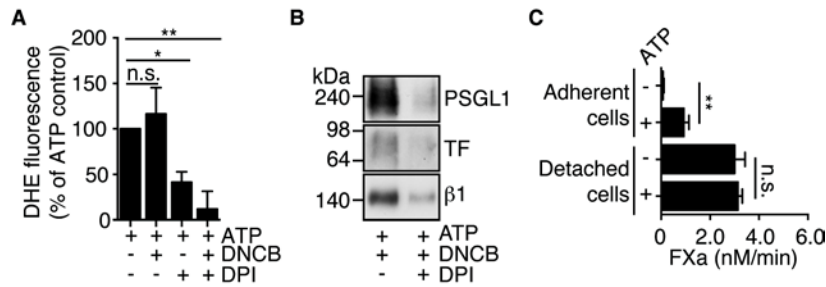


Figure S5: Control experiments for TF activation and ROS-dependent release of cell surface receptors. (A) Detection of oxidation-induced shifts in the fluorescence spectrum of dihydroethidium (DHE) showed that diphenyleneiodonium (DPI), an inhibitor of NADPH-dependent ROS production, but not DNCB prevented ATP-induced ROS formation; mean \pm SD, $n = 3$, * $P < 0.05$, ** $P < 0.01$, ANOVA (Bonferroni). (B) Western blotting for cell surface receptors on ATP-induced MP with and without DPI-treatment showed that ROS-generation was required for the release of membrane receptors from DNCB blocked macrophages. (C) TF-activity on adherent or detached cells with and without ATP-stimulation for 30 minutes determined by FXa generation showed that suppression of cellular TF activity in control cells is adhesion dependent.

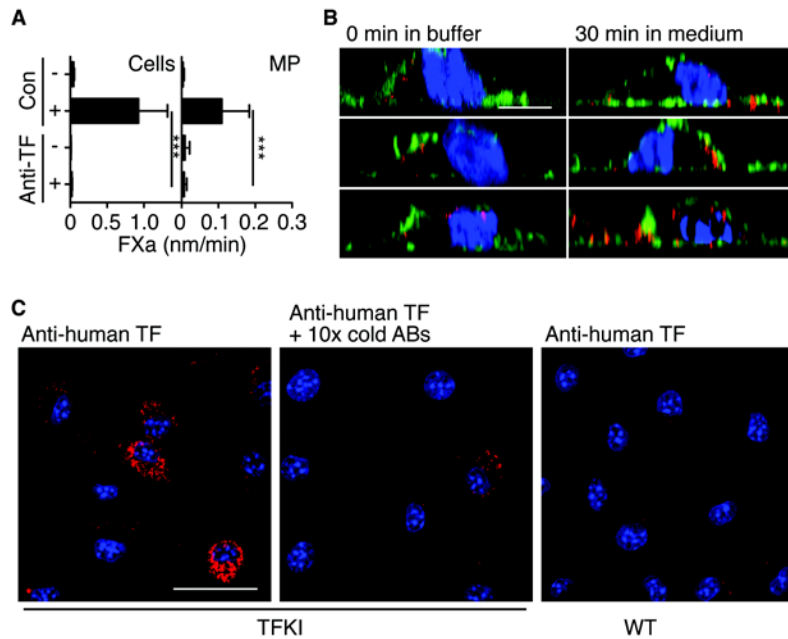


Figure S6: Control experiments for confocal imaging of TFKI macrophages. (A) FXa generation assay of cells and released MP from ATP-activated TFKI macrophages following surface staining of TF with anti-TF antibodies for 10 minutes at ambient temperature demonstrated that procoagulant TF activity on cells and MP originated from cell surface pools of TF detected by the TF-antibodies; mean \pm SD, $n = 3$, *** $P < 0.001$, ANOVA (Bonferroni). (B) Staining cells with anti-TF (red) for 10 minutes at RT followed immediately by fixation (0 min in buffer) or following incubation for 30 minutes in complete medium with serum (30 min in medium) showed that staining antibodies did not induce TF internalization. Fixed cells were counterstained with phalloidin-Alexa 488 for F-actin (green) and Hoechst for nuclei (blue). Z-section of 0.29 μm thickness were scanned on a LSM microscope; scale bar = 5 μm . (C) Specificity of TF-labeling of TFKI macrophages was verified by staining cells together with a 10-fold excess of non-labeled anti-TF antibodies (middle panel) or by staining WT macrophages expressing mouse TF with human TF-specific Alexa 647 conjugates (right panel); scale bar = 20 μm .

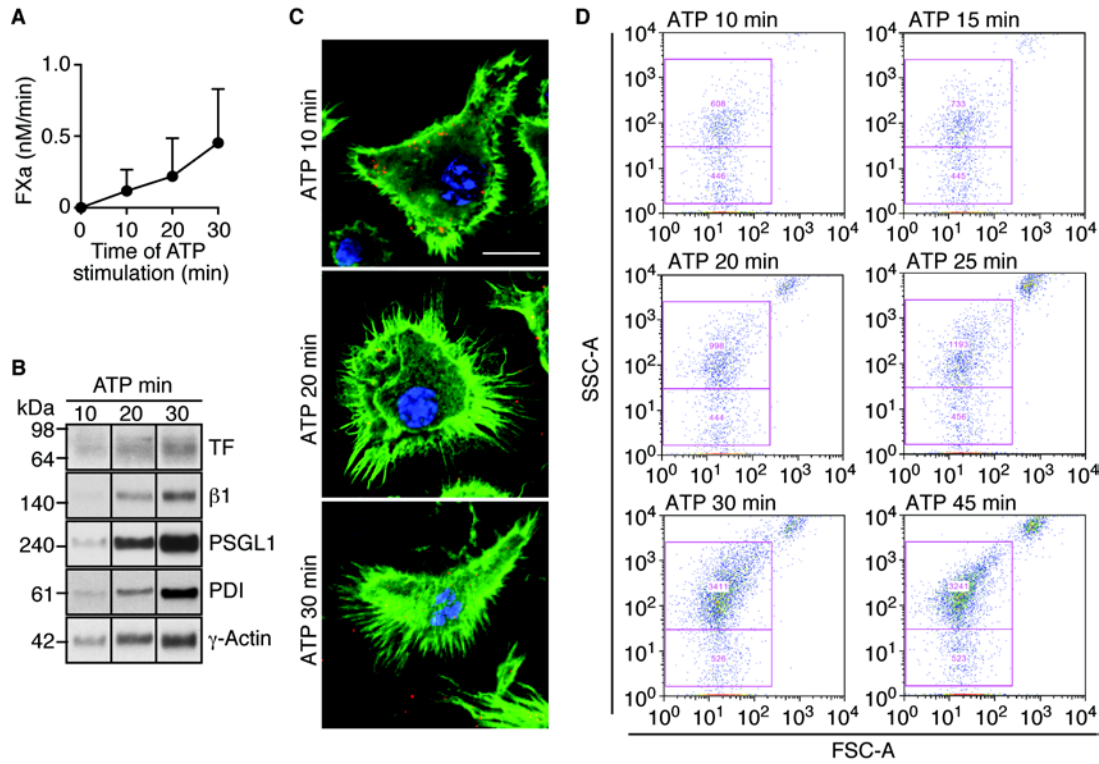


Figure S7: *Filopodia formation and procoagulant TF⁺ MP release following ATP stimulation.* Time course of (A) TF activity by FXa generation assay (mean \pm SD) and (B) antigen detection of TF, integrin β 1, PSGL1, PDI and γ -actin by Western blotting on MP after the indicated times of ATP stimulation demonstrated that MP pro-coagulant MP release coincided with (C) the translocation of TF onto filopodia visualized by confocal imaging of ATP-stimulated TFKI macrophages with anti-human TF antibody (red). Cells were stained for F-actin with phalloidin-Alexa 488 (green) and for nuclei with Hoechst (blue) after fixation; scale bar = 10 μ m. (D) FACS detection of MP from TFKI macrophages after the indicated times of ATP-stimulation.

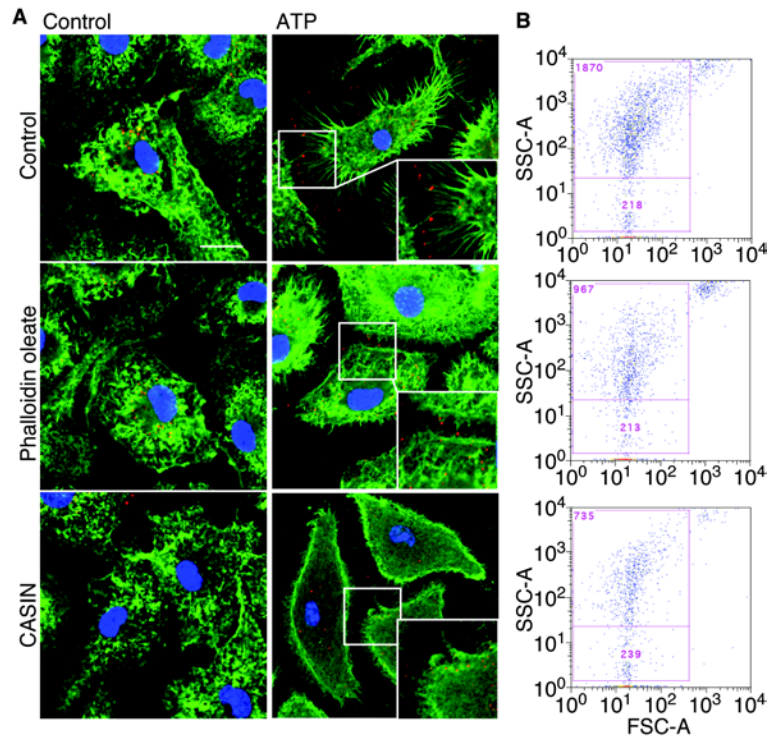


Figure S8: *Effect of inhibitors of cytoskeletal reorganization on filopodia formation and MP release.* Inhibitors of actin remodeling (phalloidin oleate) or filopodia formation (CASIN, an inhibitor of the small Rho GTPase CDC42) attenuated both filopodia formation and the release of large MP from TFKI macrophages. (A) TF staining after stimulation with ATP for 20 minutes in cell pre-treated for 20 minutes with 1 μ M phalloidin oleate, which binds F-actin and impairs cytoskeleton remodeling, or 10 μ M CASIN. Permeabilized cells were counterstained with phalloidin-Alexa 488 and Hoechst stain to visualize F-actin (green) and nuclei (blue). Representative overviews with views at higher magnification for ATP-stimulated cells are shown; scale bar = 10 μ m. (B) FACS analysis of MP released from cells activated with ATP in the presence or absence of phalloidin oleate or CASIN.

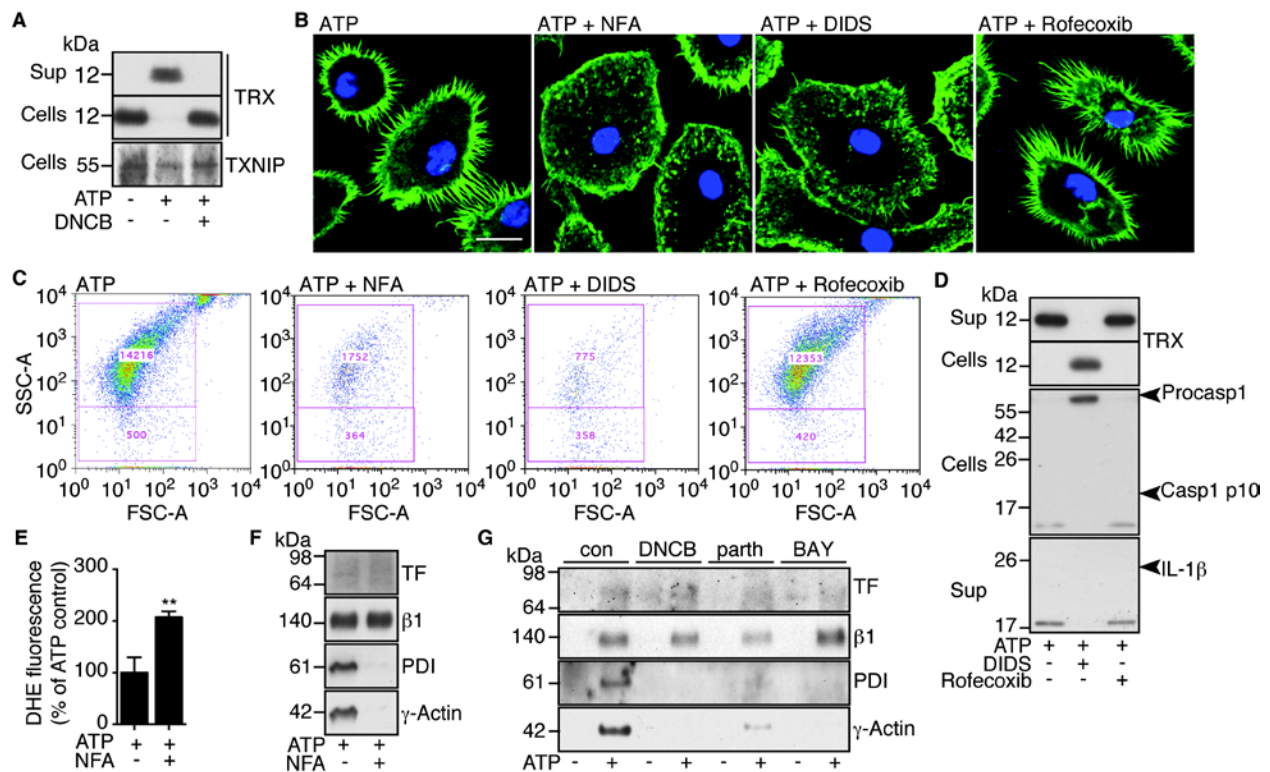


Figure S9: Control experiments for the effects of inflammasome inhibition. The following data provide supplemental information for the effects of inflammasome inhibition by specific inhibitors parthenolide (parth) and BAY 11-7082 (BAY) and endosomal ROS generation by NFA-treatment on the ATP-induced thrombo-inflammatory pathway. TFKI macrophages were used for FACS analysis and confocal imaging. (A) Western blotting of TRX and TXNIP in cells and supernatant with or without DNCB-treatment showed ATP-induced separation of cellular TRX and TXNIP dependent on TRXR activity. (B) Effect of the chloride channel blockers NFA and DIDS or the COX2 inhibitor Rofecoxib on ATP-induced filopodia formation. Cells were fixed after 20 minutes of ATP-stimulation and stained with phalloidin-Alexa 488 and Hoechst for F-actin (green) and nuclei (blue); scale bar = 10 μ m. (C) FACS characterization of MP released from cells activated with ATP with or without NFA, DIDS, or Rofecoxib incubation. Event counts are displayed in the gates of large and small MP. (D) Effect of DIDS or Rofecoxib on caspase 1 activation, release of TRX and IL-1 β processing in cells and supernatants were determined by Western blotting. (E) ROS measured by oxidation-mediated changes in DHE-fluorescence demonstrated that NFA-treatment did not inhibit overall ATP-induced ROS production. (F) Effect of NFA on MP release of TF, integrin β 1, PDI and γ -actin downstream of ATP-stimulation analyzed by Western blotting. (G) Western blotting for TF, integrin β 1, PDI and γ -actin on MP demonstrated that inhibition of inflammasome activity by parthenolide (parth) or BAY 11-7082 (BAY) resulted in a similar MP composition as inhibiting TRXR activity with DNCB.

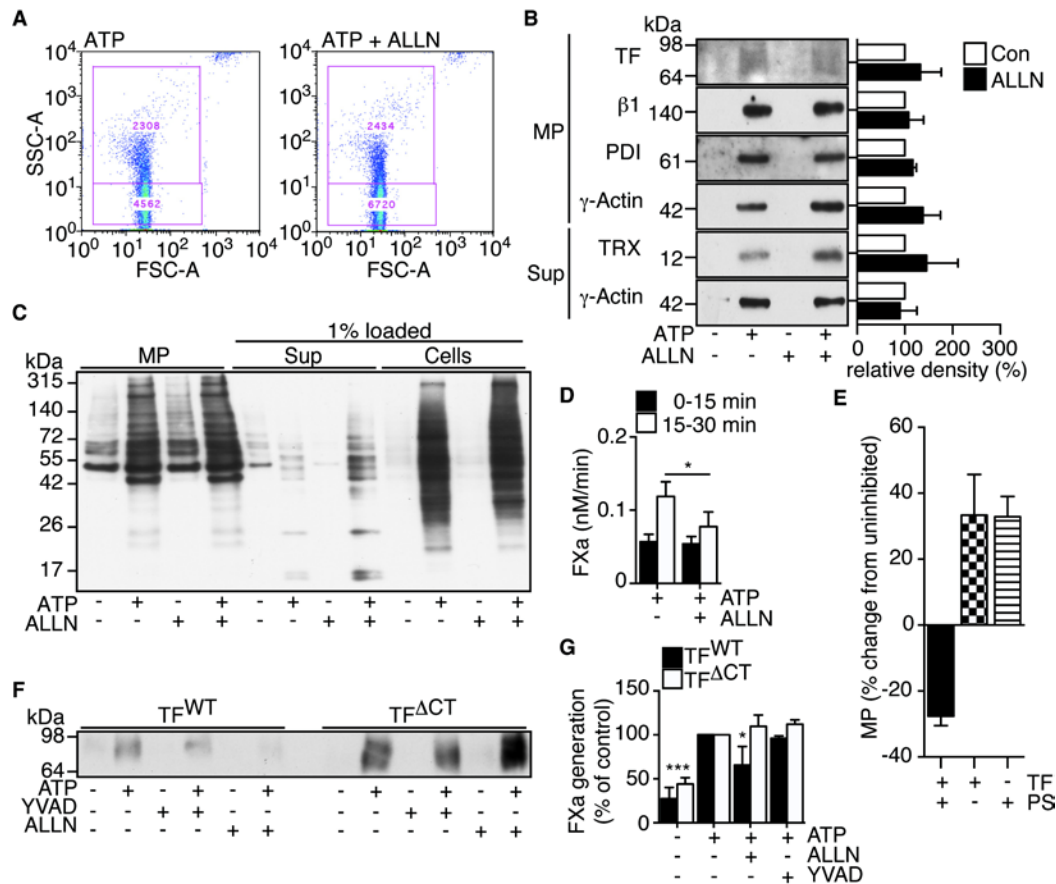


Figure S10: Effects of calpain inhibition on MP release from macrophages and smooth muscle cells. (A) FACS analysis of ATP-induced MP released from control and ALLN-treated TFKI macrophages. (B) Effects of calpain inhibition on ATP-induced release of proteins in MP and into the cell-free supernatant. Representative Western blots (left panel) and quantification (right panel) are shown; mean \pm SD, $n = 3$, n.s., t test. (C) MPB-labeling of protein free thiols in MP, cell supernatant (Sup), and cell surfaces of control and ALLN-blocked cells with or without ATP stimulation detected by streptavidin blot. (D) FXa generation assay of MP collected 0 - 15 minutes (black bars) and 15 - 30 minutes (open bars) after ATP stimulation of control or ALLN-treated cells; mean \pm SD, $n = 3$, $*P < 0.05$, ANOVA (Bonferroni). (E) PS and TF incorporation into MP from control and ALLN-treated TFKI macrophages after ATP-stimulation was analyzed by FACS. Plotted are the deviations in counts of MP in cells treated with ALLN compared to control; MP incorporating TF and PS were reduced ($P < 0.01$), MP incorporating TF or PS alone were increased ($P < 0.05$ and $P < 0.05$, respectively); $n = 3$, t test. (F) Western blot of TF on MP released from TF^{WT} or TF ^{Δ CT} smooth muscle cells with or without inhibitors ALLN and YVAD. (G) Pro-coagulant activity of MP from smooth muscle cells was determined by FXa generation assay and normalized to FXa generation by ATP-induced MP of the same genotype without inhibitors.

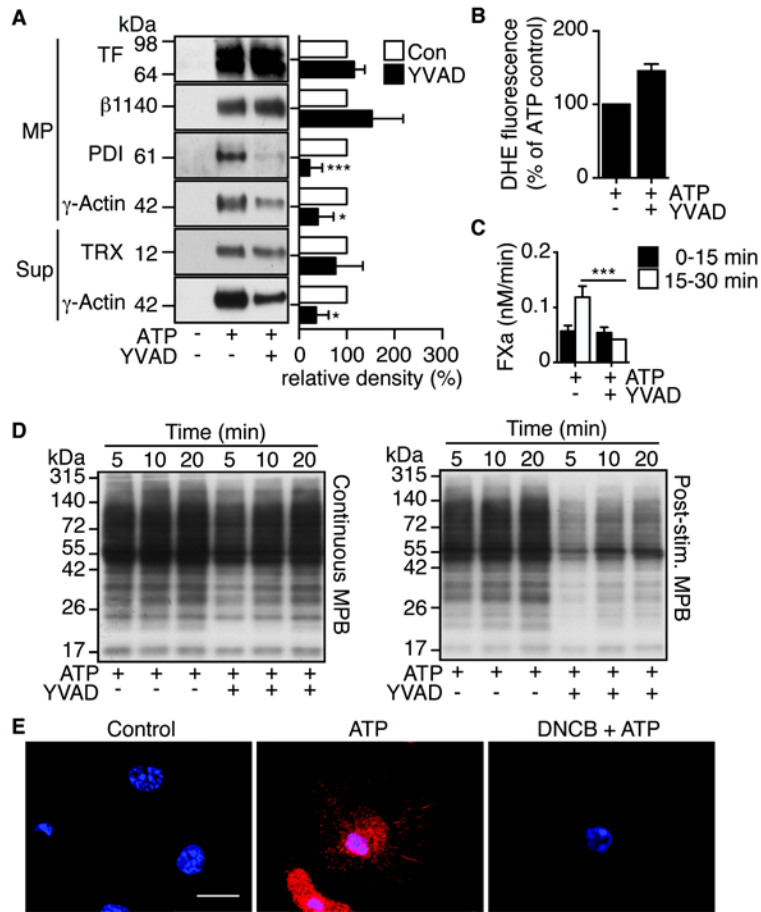


Figure S11: Control experiments for the effects of pharmacological caspase 1 inhibition. (A) Representative Western blots (left panel) and quantification (right panel) of proteins on MP and in the cell-free supernatant released from ATP-stimulated control and caspase 1-inhibited (YVAD) macrophages; mean \pm SD, $n = 3$, $***P < 0.001$, $*P < 0.05$, t test. (B) ATP-induced ROS formation in YVAD-treated cells determined by changes in DHE fluorescence. (C) Effects of YVAD treatment on FXa generation by MP collected 0 - 15 minutes (black bars) and 15 - 30 minutes (open bars) following ATP stimulation; $n = 3$, $*P < 0.05$, ANOVA (Bonferroni). (D) MPB labeling of cell surface free thiols in cells stimulated with ATP indicated that thiol exposure in caspase 1-inhibited cells (YVAD) was less stable compared to controls. MPB added at the beginning of ATP stimulation (left panel) or at the end of the experiment for post ATP-stimulation MPB labeling (right panel). (E) Confocal imaging of continuously MPB-labeled control and ATP-stimulated control and DNCB-treated cells. MPB was visualized with TexasRed-labeled streptavidin (red); scale bar = 10 μ m.

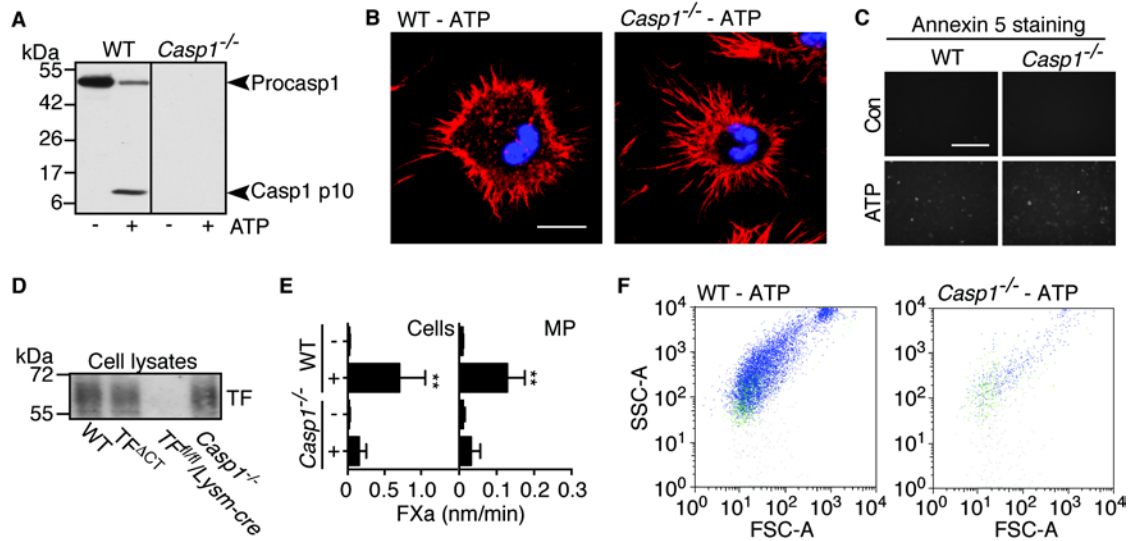


Figure S12: Experiments in macrophages from caspase 1-deficient mice. The following findings in caspase 1-deficient macrophages support the conclusion that caspase 1 is crucial for P2RX7-dependent thrombo-inflammatory MP release. (A) Western blots of caspase 1 in cell lysates of control and ATP-stimulated macrophages from WT and caspase 1-deficient (*Casp1*^{-/-}) mice. (B) ATP-induced filopodia formation in WT compared to *Casp1*^{-/-} macrophages. Cells were fixed after 20 minutes of ATP stimulation and stained with phalloidin-Alexa 647 and Hoechst for F-actin (red) and nuclei (blue); scale bar = 10 μ m. (C) Staining with annexin 5-FITC showed similar PS-exposure in response to ATP in WT and *Casp1*^{-/-} macrophages, scale bar = 10 μ m. (D) Western blot of TF demonstrated similar cellular TF expression in WT and *Casp1*^{-/-} macrophages. (E) TF activity on cells and MP of WT and *Casp1*^{-/-} macrophages determined by FXa generation assay. (F) FACS analysis revealed that ATP-stimulated *Casp1*^{-/-} macrophages did not release thrombi-inflammatory MP.

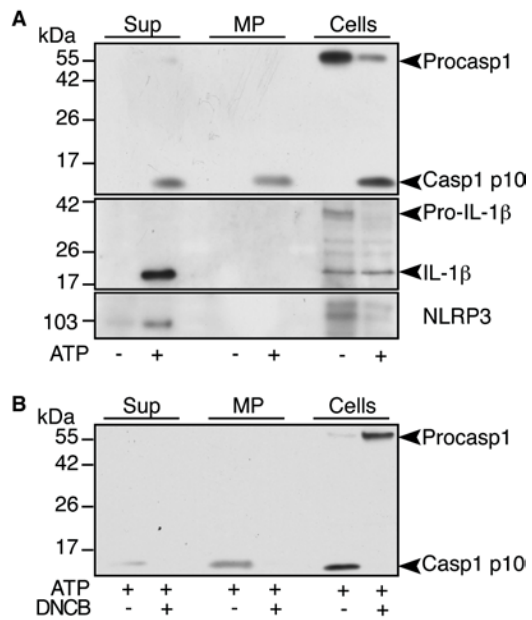


Figure S13: Detection of components of the inflammasome in cells, MP and MP-free cell supernatants. (A) Shown are Western blots of control and ATP-stimulated macrophages (5 mM, 30 minutes) for caspase 1, IL-1 β and NLRP3 in cell lysates, MP and MP-free supernatants. (B) Detection of caspase 1 in cell fractions of control and DNCB-treated macrophages upon ATP-stimulation shows that release of caspase 1 on MP and into the cell supernatant is dependent on functional TRXR.

Supplemental Movies

Online supplemental movies provide 3-dimensional reconstructions for macrophage staining. TFKI cells were labeled with human TF-specific Alexa 647 conjugates (red) prior to stimulation for 20 minutes in BSS buffer. Cells were counterstained with phalloidin-Alexa 488 (green), and Hoechst (blue) for F-actin and nuclei, respectively. Z-stacks were composed from optical slices of 0.29 μm thickness using Imaris (Bitplane, South Windsor, CT) image analysis software.

Movie S1: control cells, related to figure 3.

Movie S2: ATP-stimulated (5 mM) cells, related to figure 3.

Movie S3: DNCB-treated (30 μM) cells without ATP stimulation, related to figure 3.

Movie S4: DNCB-treated (30 μM) cells with ATP stimulation (5 mM), related to figure 3.

Movie S5: YVAD-treated (10 μM) cells without ATP stimulation, related to figure 8.

Movie S6: YVAD-treated (10 μM) cells with ATP stimulation (5 mM), related to figure 8.

Supplemental Table

kDa	Protein identified	Cytoskeleton and MP release
51	Angiogenin inhibitor 1	Angiogenin promotes actin polymerization
41	γ -actin	Structural component
39	Annexin A1	Binds PS and actin; released from macrophages and epithelial cells dependent on actin dynamics
36	Annexin A5	Binds PS and actin
33	Purine nucleoside phosphorylase	Associated with cytoskeleton and released on MP from cancer and immune cells
28	14-3-3 ζ	Mediates integrin-induced activation of CDC42 and cytoskeletal reorganization

Table S1: *Identification of 6 prominent proteins released from ATP-stimulated cells by mass spectrometry and their association with the cytoskeleton and MP release.*

Supplemental References

1. Melis,E., Moons,L., De Mol,M., Herbert,J.M., Mackman,N., Collen,D., Carmeliet,P., and Dewerchin,M. 2001. Targeted deletion of the cytosolic domain of tissue factor in mice does not affect development. *Biochem. Biophys. Res. Commun.* **286**:580-586.
2. Pawlinski,R., Tencati,M., Holscher,T., Pedersen,B., Voet,T., Tilley,R.E., Marynen,P., and Mackman,N. 2007. Role of cardiac myocyte tissue factor in heart hemostasis. *J Thromb Haemost.* **5**:1693-1700.
3. Kuida,K., Lippke,J.A., Ku,G., Harding,M.W., Livingston,D.J., Su,M.S., and Flavell,R.A. 1995. Altered cytokine export and apoptosis in mice deficient in interleukin-1 beta converting enzyme. *Science* **267**:2000-2003.
4. Snyder,L.A., Rudnick,K.A., Tawadros,R., Volk,A., Tam,S.H., Anderson,G.M., Bugelski,P.J., and Yang,J. 2008. Expression of human tissue factor under the control of the mouse tissue factor promoter mediates normal hemostasis in knock-in mice. *J Thromb Haemost.* **6**:306-314.
5. Furlan-Freguia,C., Marchese,P., Gruber,A., Ruggeri,Z.M., and Ruf,W. 2011. P2X7 receptor signaling contributes to tissue factor-dependent thrombosis in mice. *J Clin Invest.* **121**:2932-2944.
6. Sevinsky,J.R., Rao,L.V.M., and Ruf,W. 1996. Ligand-induced protease receptor translocation into caveolae: A mechanism for regulating cell surface proteolysis of the tissue factor-dependent coagulation pathway. *J. Cell Biol.* **133**:293-304.
7. Doshi,N., Orje,J.N., Molins,B., Smith,J.W., Mitragotri,S., and Ruggeri,Z.M. 2012. Platelet mimetic particles for targeting thrombi in flowing blood. *Adv. Mater.* **24**:3864-3869.
8. Ruf,W., and Edgington,T.S. 1991. An anti-tissue factor monoclonal antibody which inhibits TF:VIIa complex is a potent anticoagulant in plasma. *Thromb. Haemost.* **66**:529-533.
9. Kirkpatrick,D.L., Kuperus,M., Dowdeswell,M., Potier,N., Donald,L.J., Kunkel,M., Berggren,M., Angulo,M., and Powis,G. 1998. Mechanisms of inhibition of the thioredoxin growth factor system by antitumor 2-imidazolyl disulfides. *Biochem. Pharmacol.* **55**:987-994.